Mass spectrometric identification of [4Fe-4S](NO)$_x$ intermediates of nitric oxide sensing by regulatory iron-sulfur cluster proteins

Jason C. Crack[a] and Nick E. Le Brun[a]

[a] J. C. Crack and N. E. Le Brun
Centre for Molecular and Structural Biochemistry, School of Chemistry, University of East Anglia, Norwich Research Park, Norwich, NR4 7TJ, UK
Email: n.le-brun@uea.ac.uk.

Supporting information for this article is available on the WWW under http://.

Abstract

Nitric oxide (NO) can function as both a cytotoxin and a signalling molecule. In both cases, reaction with iron-sulfur (Fe-S) cluster proteins plays an important role because Fe-S clusters are reactive towards NO and so are a primary site of general NO-induced damage (toxicity). This sensitivity to nitrosylation is harnessed in the growing group of regulatory proteins that function in sensing of NO via an Fe-S cluster. Although information about the products of cluster nitrosylation is now emerging, detection and identification of intermediates remains a major challenge, due to their transient nature and the difficulty in distinguishing spectroscopically similar iron-NO species. Here we report studies of the NO-sensing Fe-S cluster regulators NsrR and WhiD using non-denaturing mass spectrometry, in which non-covalent interactions between the protein and Fe/S/NO species are preserved. The data provide remarkable insight into the nitrosylation reactions, permitting identification, for the first time, of protein-bound mono-, di- and tetra-nitrosyl [4Fe-4S] cluster complexes ([4Fe-4S](NO), [4Fe-4S])$(NO)_2$ and [4Fe-4S]$(NO)_4$) as intermediates along pathways to formation of product Roussin's red ester (RRE) and Roussin's black salt (RBS)-like species. The data allow the nitrosylation mechanisms of NsrR and WhiD to be elucidated and clearly distinguished.

Introduction

The lipophilic radical molecule nitric oxide (NO) fulfils multiple functions in biology. In plants and animals, it functions as a key signalling molecule, leading, for example, to vascular smooth muscle relaxation and increased blood flow in animals. It also functions as a neurotransmitter and more generally in neuronal activity in animals, and as a cytotoxin, which is generated in macrophages during the first immune response against invasion by microbes.[1] Its importance in biology is underpinned by its chemistry; its radical nature means that it is highly reactive and readily undergoes both redox and ligand binding reactions.[2]

Iron-sulfur (Fe-S) cluster-containing proteins play central roles in many biochemical processes, from respiration and photosynthesis, to catalysis and DNA replication. In many cases, the clusters are susceptible to degradation, reflecting their inherent reactivity towards gaseous molecules such as O_2 and NO.[2b, 2c] Hence, Fe-S proteins are very likely primary targets of NO toxicity. Several bacterial NO sensor proteins contain an Fe-S cluster.[2b, 3] These include NsrR and WhiB-like (Wbl) family proteins. NsrR is a member of the widespread Rrf2 family. It binds a [4Fe-4S] cluster and in this form is able to bind the promoter regions of NsrR-regulated genes. Reaction with NO leads to loss of DNA binding, a process that underpins its function of coordinating the cell's response to nitrosative stress.[4] It is widely distributed amongst bacteria, including several pathogens that must withstand host-generated nitrosative stress in order to establish infection.[5] Recently, the structure of [4Fe-4S] NsrR dimer was solved, revealing a DNA-binding domain, which includes a winged helix-turn-helix motif, connected to a dimerization helix via a loop containing three conserved Cys residues. The mode of cluster coordination is unique, as it is ligated by the three Cys residues from one monomer and an Asp residue from the N-terminus of the other[6] (Fig. 1A). The structure of apo-NsrR revealed a cluster-dependent movement of the DNA recognition helix, demonstrating how reaction with NO likely modulates DNA-binding.

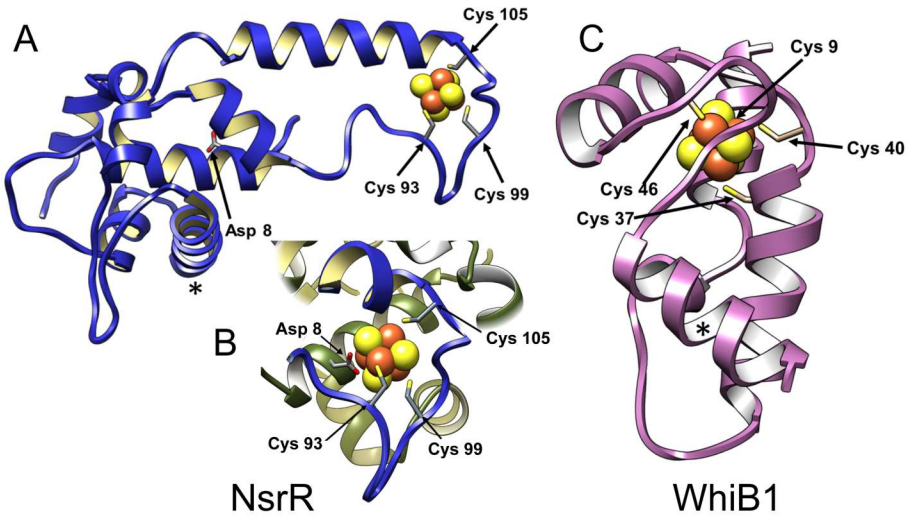

Figure 1. Structures of *S. coelicolor* [4Fe-4S] NsrR and *M. tuberculosis* [4Fe-4S] WhiB1. (A) Cartoon diagram showing the X-ray structure of one subunit of the NsrR homodimer.[6] (B) Closer view of the [4Fe-4S] cluster showing how Asp8 from the second monomer coordinates the cluster of the first. (C) Cartoon diagram of the NMR structure of WhiB1 with its cluster coordinated by four Cys residues.[7] Iron and sulfide are shown in red and yellow, respectively. The DNA recognition helix of each protein is indicated by an asterisk.

Members of the WhiB-like (Wbl) family, which are also [4Fe-4S] proteins, are found exclusively in Actinobacteria. This phylum includes the *Streptomycetes*, a group of non-motile, spore forming, soil dwelling bacteria, that are the most abundant source of clinically important antibiotics, and *Mycobacteria*, which include *M. tuberculosis*, the causative agent of tuberculosis. Wbl proteins carry out a range of important functions. In *Streptomyces*, WhiB and WhiD are required for sporulation,[8] while WblA and WblC are involved in antibiotic production and developmental processes[9] and antibiotic resistance,[10] respectively. WhiB was recently shown to exert its regulatory effects in conjunction with WhiA, a protein that belongs to the homing endonuclease family but which has lost the catalytic nuclease residues.[8d] In *M. tuberculosis*, Wbl proteins are important for the long term persistence of this pathogen within its host despite the low nutrient and oxidative nature of the granulome, as well as its remarkable tolerance to a wide range of antibiotics.[10-11] It has been shown that *M. tuberculosis* accumulates tri-acylglycerol in response to hypoxia and NO exposure,[12] a process that is regulated by WhiB3 (the *M. tuberculosis* homologue of *S. coelicolor* WhiD) in response to activated macrophages.[13] Recently, the first structure of a Wbl protein, that of *M. tuberculosis* [4Fe-4S] WhiB1, was reported. This revealed a four-helix bundle protein with the [4Fe-4S] cluster coordinated by the four conserved Cys residues[7] (Fig. 1B). The same study showed that it forms a stable complex with the sigma factor SigA that is dependent on the cluster; reaction with NO led to dissociation of the complex and a form of WhiB1 that can bind its own promoter.[7, 14] Other *M. tuberculosis* Wbl proteins have been shown to interact with SigA, suggesting that Wbl proteins commonly function together with partner proteins.[15]

The mechanisms by which Fe-S regulatory proteins react with NO are not well characterized. Recent advances in techniques for Fe-S protein preparation and handling have facilitated studies by a variety of methods that have demonstrated that multinuclear iron species similar to the well known inorganic complexes Roussin's Red Ester (RRE; $[Fe_2(NO)_4(SR)_2]$) and Roussin's Black Salt (RBS; $[Fe_4(NO)_7(S)_3]$)[16] (see Fig. S1) are major products.[17] In some cases, di-nitrosyl iron complexes (DNICs, $[Fe(NO)_2(SR)_2]$) are also produced, however, it is clear that in general these are not the major products.[2b] In the case of NsrR and WhiD, studies employing the novel iron-specific technique nuclear resonance vibrational spectroscopy (NRVS) showed that nitrosylation results in a mixture of RRE and RBS-like species[18] and a very recent study employing liquid chromatography electrospray ionisation mass spectrometry (LC ESI-MS)[19] provided the first unambiguous evidence of RRE and a persulfide form ($[Fe_2(NO)_4$(S-Cys)(Cys)]) as products of nitrosylation in NsrR.

These iron-nitrosyl species involve multiple NO molecules, suggesting a complex mechanism for nitrosylation. Indeed, studies of a range of NO sensing [4Fe-4S] regulatory proteins, including *S. coelicolor* WhiD and NsrR,[17d, 20] and *Escherichia coli* FNR,[17e] showed that reaction with NO is a remarkably rapid and complex multi-step process involving up to ~8 NO molecules per cluster. Despite these recent advances, understanding the mechanism of this biologically important reaction remains a major challenge, particularly because of the difficulty in observing and identifying intermediates in the nitrosylation reaction.

ESI-MS utilising solution and ionization conditions under which proteins remain folded enables accurate mass detection of intact proteins and protein complexes, and has been used extensively to study protein-protein interactions, interactions of proteins with drug molecules, oligonucleotides, carbohydrates, and lipids, as well as protein structural changes.[21] ESI-MS of iron-sulfur cluster proteins, where the cluster remains bound following vapourisation/ionisation, has also been shown to be a valuable technique,[22] and recently provided detailed mechanistic information of the O_2-sensing reaction of the [4Fe-4S] cluster

binding FNR regulator[23] and evidence of NO-binding to the [2Fe-2S] clusters of human Miner2 and variant forms of Miner1 and MitoNEET.[24]

Here, we report the application of ESI-MS under non-denaturing conditions to studies of the reactions of the [4Fe-4S] clusters of NsrR and WhiD with NO. The data reveal, in remarkable detail, intermediates and products of the reaction of the clusters with NO and enable the nitrosylation mechanisms of the two regulators to be distinguished.

Results

ESI-MS detection of mono-nitrosylated [4Fe-4S], the first intermediate of the reactions of NsrR with NO

ESI-MS under non-denaturing conditions was used to study the reaction of [4Fe-4S] NsrR with NO. The m/z spectrum (Fig. S2) comprised two regions corresponding to monomeric and dimeric forms of NsrR, as previously reported.[4a, 6] The deconvoluted MS spectrum of [4Fe-4S] NsrR revealed broad peaks at ~34942, 35294, and 35646 Da corresponding to dimeric apo-NsrR (see Table 1 for a comparison between observed and predicted mass) and dimeric NsrR containing one (35294 Da) and two clusters (35646 Da), respectively, see Fig. S3. The intensity of the peaks due to these dimeric forms was relatively low, possibly because the protein-protein interactions that mediate dimerization do not efficiently survive the ionization process. Higher intensity and well resolved peaks were observed in the monomer region, as previously reported[4a, 6] (Fig. 2A). This contained a major peak due to apo-protein at 17,472 Da (predicted mass 17,474 Da, see Table 1), along with small amount of NsrR with sulfur adducts at +32 and +64 Da. The second major species was [4Fe-4S] NsrR, giving a peak at 17,824 Da (predicted mass 17,824 Da), along with a sodium adduct at +22 Da. In order to assist in the assignment of species, NsrR was generated containing ^{34}S and $^{57}Fe/^{34}S$ isotopes within the [4Fe-4S] cluster. As expected, for the ^{34}S-substituted cluster, a +8 Da mass shift was observed, and a +12 Da shift was observed for the $^{57}Fe/^{34}S$-substituted cluster, see Fig. 2B.

Addition of NO resulted in the decay of the [4Fe-4S] peak of NsrR and the formation of a new peak at +30 Da (Fig. 2C and D, Table 1). This is consistent with the addition of a single NO molecule to the [4Fe-4S] cluster ([4Fe-4S](NO)); Fig. 2C). Analysis of $^{57}Fe/^{34}S$ substituted [4Fe-4S] NsrR revealed clear formation of the same +30 Da species as observed for the natural abundance (predominantly $^{56}Fe/^{32}S$) cluster but shifted by +12 Da, see Fig. 2D. This demonstrates that the +30 Da peak results from the mono-nitrosyl cluster species, rather than, for example, $[4Fe\text{-}3S](NO)_2$. At natural abundance, the mass difference between these species ([4Fe-4S](NO) versus $[4Fe\text{-}3S](NO)_2$) would be difficult to unambiguously distinguish. However, for the heavy cluster, the mass difference between these species is larger and the Fe/S content is readily determined from the isotope shift. The peak due to [4Fe-4S](NO) initially increased in intensity before decaying away above ~3 NO per cluster (Fig. 2C and E). The [4Fe-4S](NO) complex of the $^{57}Fe/^{34}S$ cluster also behaved as an intermediate in that it formed and then decayed (Fig. S4), though with slightly different decay properties to the natural abundance form. These data identify, for the first time, the initial NO adduct of a regulatory protein-bound Fe-S clusters undergoing nitrosylation.

Addition of NO also resulted in changes in the +60 Da region. These are somewhat obscured by an unknown adduct of [4Fe-4S] NsrR at +58 Da that is present before the addition of NO (Fig. 2C). A small shift of the peak from +58 to 60 Da was observed along with an increase in intensity as NO was added, such that at 3.9 NO:[4Fe-4S] cluster, it was at least as intense as the [4Fe-4S](NO) peak and significantly more intense than the [4Fe-4S] peak.

Above 4 NO:[4Fe-4S], the species decayed away and we conclude that this very likely corresponds to the di-nitrosyl species, [4Fe-4S](NO)$_2$. An unambiguous assignment could not be made because this adduct was either not formed at significant abundance or obscured by a sodium adduct of [4Fe-4S](NO) in ^{57}Fe/^{34}S spectra (Fig. S4).

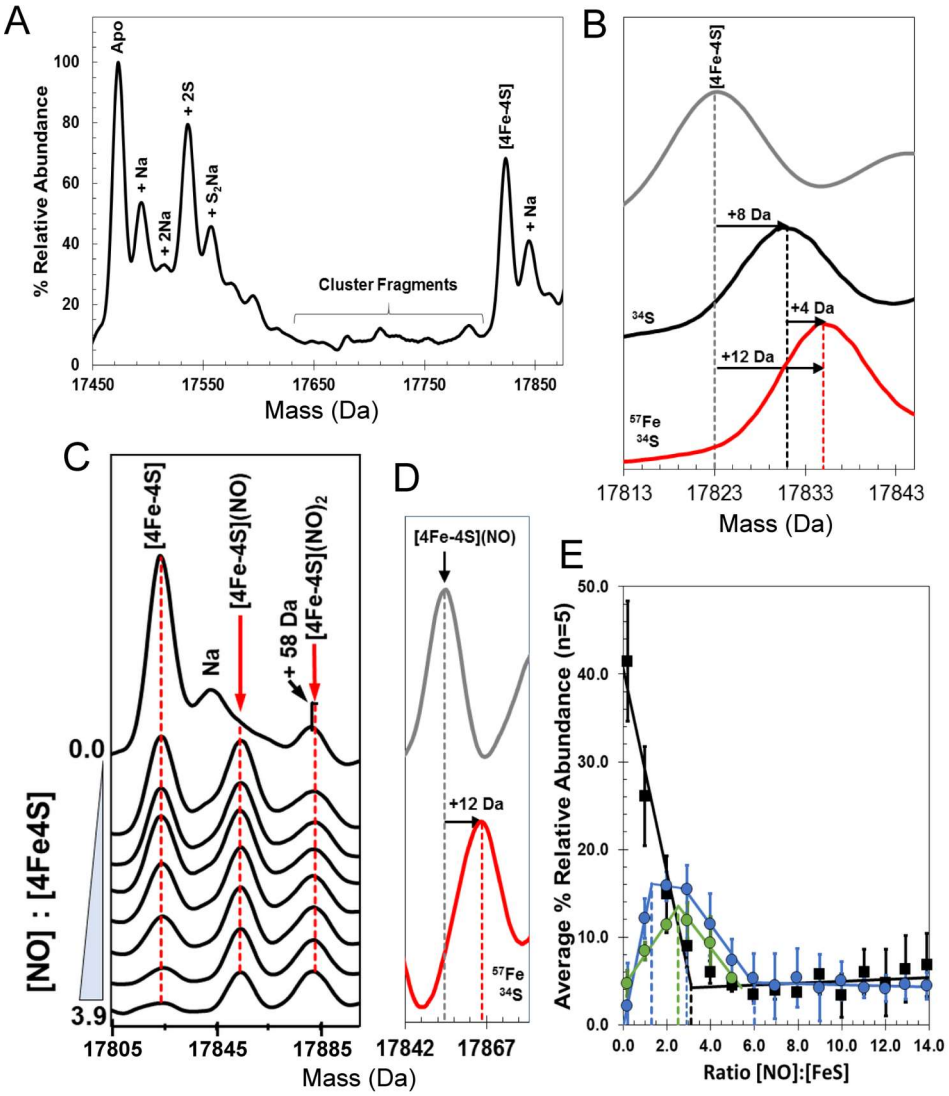

Figure 2. Detection of mono- and di-nitrosyl complexes of [4Fe-4S] NsrR, the first intermediates of nitrosylation. (A) Non-denaturing ESI-MS of [4Fe-4S] NsrR. The sample contained a mixture of apo- and [4Fe-4S] NsrR. Na and S adducts of apo- and [4Fe-4S] NsrR were observed, as indicated. Adducts between 17650 – 17791 Da correspond to cluster breakdown products. (B) [4Fe-4S] region of the spectrum of natural abundance and isotopically substituted NsrR, as indicated. (C) An aliquot of DTPA NONOate (0.76 mM final concentration) was added to 7.0 μM [4Fe-4S] NsrR and incubated at 20 °C, releasing 0.21 [NO]:[FeS] per 5 min. Exposure to NO resulted in the transient formation of single and double NO adducts (+30 and +60 Da) of the [4Fe-4S] cluster). (D) The mono-nitrosyl region of [4Fe-4S] NsrR containing natural abundance iron and sulfur (principally ^{56}Fe, ^{32}S, grey line) and ^{57}Fe, ^{34}S (red line). Attempts to measure the isotope shift were unsuccessful due to interference from sodium adducts of the mono-nitrosyl form. (E) Average (n=5) percentage relative abundance of [4Fe-4S] (black squares) and single NO adduct (blue circles) plotted as a function of the [NO]:[FeS] ratio. Error bars represent standard deviation. Solid lines indicate phases of the reaction, with break points indicated by vertical broken lines.

Table 1. Predicted and observed masses of proteins and protein-bound Fe/S/NO species.

Protein species	Predicted mass (Da)	Average observed mass (Da)[a]	ΔMass (Da)[b]	^{57}Fe and ^{34}S Isotope shift (Da)
NsrR				
Apo-NsrR	17,474	17,472	-2	-
$[4Fe\text{-}4S]^{2+}$	17,824	17,824	0	+12
$[4Fe\text{-}4S]^{2+}(NO)$	17,854	17,854	0	+12
Iron-nitrosyls[c]				
DNIC				
$[Fe(NO)_2]^{1+}$	17,589	17,588	-1	+1
$[Fe(NO)_2(NH_4)]^{2+}$	17,606	17,606	0	+1
RRE				
$[Fe_2(NO)_4(S^0)]^{2+}$	17,736	17,736	0	+4
RBS-like[d]				
$[Fe_4S_3(NO)_3]^x$	17,875 – 17,883	17,881		+10
$[Fe_4S_3(NO)_4]^x$	17,906 – 17,914	17,912		+10
$[Fe_4S_3(NO)_5]^x$	17,937 – 17,945	17,941		+10
$[Fe_4S_3(NO)_6]^x$	17,967 – 17,976	17,972		+10
$[Fe_4S_3(NO)_5(O)]^x$	17,953 – 17,961	17,957		*n.d*
$[Fe_4S_3(NO)_6(O)]^x$	17,983 – 17,992	17,985		*n.d*
$[Fe_4S_2(NO)_7(O)(Na)]^x$	18,003 – 18,011	18,008		+8
WhiD				
Apo-WhiD	14,159	14,028	-131	-
ΔMet-WhiD	14,028	14,028	0	-
$[4Fe\text{-}4S]^{2+}$	14,378	14,377	-1	+11
$[4Fe\text{-}4S]^{2+}(NO)$	14,408	14,408	0	+11
$[4Fe\text{-}4S]^{2+}(NO)_2$	14,438	14,437	-1	+12
$[4Fe\text{-}4S]^{2+}(NO)_4$	14,498	14,496	-2	+11
RBS-like[c,e]				
$[Fe_4S_3(NO)_7]^x$	14,553 – 14,559	14,555		+10
$[Fe_4S_3(NO)_7(O)]^x$	14,569 – 14,575	14,570		+10

[a] The average observed mass was derived from at least four independent experiments, with SD of ±1 Da.

[b] The difference between the average observed and predicted mass.

[c] Iron nitrosyl species formulae refer only to the non-protein components. Here, the predicted mass depends on the charge contributed by the iron-nitrosyl and the resulting charge compensation of iron-nitrosyl binding. The overall +2 charge is compensated for by coordination to deprotonated bridging thiolates (total =-2), giving an overall charge of zero for the protein-bound species. Because the thiolates are part of the protein, they are not shown here.

[d] The charges of RBS-related species are not known. A range of masses can be predicted (as indicated) by assuming that (i) the total charge on the four irons is +10 (as it is in the starting cluster) or +12 (as it is in RBS where the irons are bound by NO^-); (ii) the NOs are present as NO^-; and, (iii) that the sulfurs present are either S^{2-} or S^0. Note that an increase in overall charge, due to iron or sulfide oxidation, results in a decrease in the predicted mass because fewer protons are required to achieve the observed charge of each ion in the m/z spectrum (see methods).
[e] The charges of RBS-like species are not known, but a range of masses can be predicted (as indicated) by assuming that (i) the total charge on the four irons is +12 (as it is in RBS itself); (ii) the NOs are present as NO^-; and, (iii) that the sulfurs present are either S^{2-} or S^0. See footnote (d) for further explanation.

ESI-MS detection of mono-, di- and tetra-nitrosylated [4Fe-4S] cluster intermediates in WhiD

ESI-MS under non-denaturing conditions was also used to study the reaction of [4Fe-4S] WhiD with NO. The m/z spectrum (Fig. S5) comprised a single region due to monomeric WhiD, consistent with previous solution studies.[8c] The deconvoluted spectrum, Fig. 3A, revealed the presence of the [4Fe-4S] cluster bound protein at 14,378 Da (Table 1), 131 Da lower than predicted, indicating N-terminal methionine excision. Low intensity peaks due to sodium and sulfur adducts were also observed. Essentially no apo-WhiD was detected owing to the high proportion of cluster-bound protein as isolated, and the greater stability of the protein in the acetate buffer compared to NsrR. A $^{57}Fe/^{34}S$-substituted [4Fe-4S] cluster gave a mass shift of ~+11 Da, consistent with the complete, or near complete, substitution of natural abundance iron and sulfur with ^{57}Fe and ^{34}S, see inset Fig. 3A.

For WhiD, addition of NO also led to the loss of the [4Fe-4S] peak. However, the decay behaviour was very different to that observed for NsrR. For WhiD, the cluster peak decayed away gradually throughout the titration, being lost entirely only above ≥10 NO per cluster, see Fig. 3B. These observations are entirely consistent with previous solution studies showing that WhiD reacts in a more concerted/cooperative manner with NO than does NsrR,[17d, 20] and with ESI-MS studies of *M. tuberculosis* WhiB1 and its complex with SigA in response to NO,[7?] which was also detectable up to the end of the full reaction with NO. Thus, unreacted [4Fe-4S] WhiD persists even when multiple NO molecules per cluster have been added.

Along with the decay of the [4Fe-4S] peak, a new peak at +30 Da was also detected (Table 1), although this was less clear than in the NsrR spectrum because of an overlapping peak due to a sulfur adduct at +32 Da. Similar measurement with a $^{57}Fe/^{34}S$-substituted form gave a gradual mass shift from +34 Da (for the ^{34}S adduct) to +30 Da as NO was added, before the peak decayed away at ≥10 NO per cluster, see Fig. 3B.

In addition to the +30 Da peak, a peak at +60 Da was observed in WhiD mass spectra (Fig. 3B and Table 1). This was initially obscured by a +62 Da peak (due to an unknown adduct species), but as the [4Fe-4S] peak decayed, so did the adduct peak, leaving the +60 Da peak clearly visible. Like the mono-nitrosyl adduct peak, the +60 Da persisted over a broad range of NO ratios, but decayed away ≥10 NO per WhiD [4Fe-4S] cluster, consistent with its formation via the binding of a second NO to [4Fe-4S](NO) to generate the di-nitrosylated cluster, $[4Fe\text{-}4S](NO)_2$. Isotope shift analysis (natural abundance versus $^{57}Fe/^{34}S$ cluster) revealed a mass difference of ~+12 Da (Fig. 3C), demonstrating that the +60 Da peak results from the cluster di-nitrosyl species.

A further peak, at +120 Da, corresponding to a tetra-nitrosylated cluster, $[4Fe\text{-}4S](NO)_4$, was also observed (Fig. 3D, Table 1). This was shifted by +~11 Da in the $^{57}Fe/^{34}S$ substituted sample (Fig. 3E), consistent with the assignment of all of the additional mass to NO binding. Intensity due to this species was observed early in the NO titration and persisted

until ~10 NO:[4Fe-4S], again consistent with the concerted nature of the WhiD nitrosylation reaction.

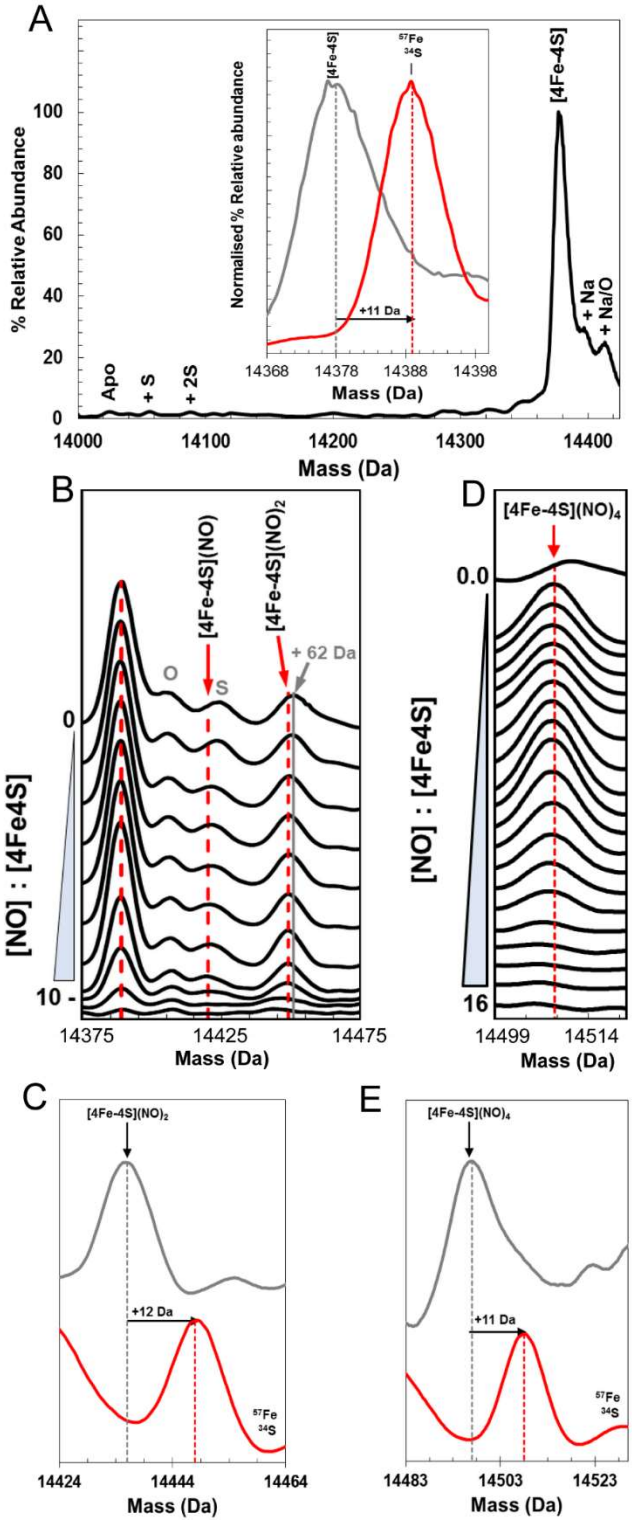

Figure 3. Detection of mono-, di- and tetra-nitrosyl forms of [4Fe-4S] WhiD. (A) Non-denaturing ESI-MS of WhiD. The spectrum contained essentially only cluster bound WhiD, reflecting the ease of ionization of this form of the protein. Na and O adducts of the [4Fe-4S] form were also observed. Inset, [4Fe-4S] region of the spectrum of natural abundance (principally ^{56}Fe, ^{32}S) and isotopically substituted (^{57}Fe, ^{34}S) WhiD, as indicated. (B) and (C) An aliquot of DTPA NONOate (1.05 mM final concentration) was added to 9.4 μM $^{57}Fe/^{34}S$ [4Fe-4S] WhiD and incubated at 37 °C, releasing 1.73 [NO]:[4Fe-4S] per 5 min. Exposure to NO led to the transient formation of single (+30 Da) and double (+60 Da) NO adducts

(B) and a tetranitrosyl adduct at +120 Da (C) of the [4Fe-4S] cluster, as indicated. (D) and (E) Comparisons of nitrosyl species formed during nitrosylation of the natural abundance and isotopically substituted forms of [4Fe-4S] WhiD. Peaks at +60 Da and +120 Da were shifted by ~+12 and ~11 Da, respectively for the $^{57}Fe/^{34}S$ cluster demonstrating that these are due to $[4Fe\text{-}4S](NO)_2$ and $[4Fe\text{-}4S](NO)_4$, respectively.

ESI-MS detection of DNIC, RRE and RBS-like products

For NsrR, a tetra-nitrosyl cluster intermediate was not observed in the NO titration followed using ESI-MS. This is consistent with recent studies of the effects of NO on binding of [4Fe-4S] NsrR to DNA, which showed that binding to the *hmpA2* promoter was abolished at >2 NO per cluster,[20] and with LC-MS studies that showed cluster sulfide is released above ~2 NO per cluster,[19] resulting in cluster degradation. However, a range of iron-nitrosyl species were detected at higher levels of NO, see Fig. 4. These occurred in mass regions that correspond to DNICs, RRE and RBS-like protein adducts (Fig. 4A). A peak was observed at 17,588 Da corresponding to the formation of a DNIC, $[Fe(NO)_2(Cys)_2]$, species (Table 1). Ammonium and ammonium/sodium adducts were also observed (Fig. 4B) and, as expected, each of these species exhibited the same intensity profile as the parent $[Fe(NO)_2(Cys)_2]$ species. Consistent with this assignment, $^{57}Fe/^{34}S$ isotope substitution resulted in a shift of +1 Da (Fig. 4E). Though these DNICs began to form at low ratios of NO:[4Fe-4S], the majority of the intensity was observed at [NO]:[4Fe-4S] ratios of ≥6 (Fig. 4D), indicating that the DNIC is primarily a product of the nitrosylation reaction.

In the RRE region, a persulfide coordinated RRE ($[Fe_2(NO)_4(S)]$) species was observed at 17,736 Da (Table 1). $^{57}Fe/^{34}S$ isotope substitution resulted in a shift of +4 Da, as expected (Fig. 4E). Mono- and di-sodium adducts were also detected (Fig. 4B) and all of these exhibited the same intensity behaviour, increasing in concentration markedly at >6 NO per cluster and reaching a maximum at ~9 per cluster (Fig. 4D). RRE species lacking the persulfide were not detected with significant intensity. These data are broadly consistent with LC-MS data, which showed RRE and persulfide RRE species accumulating at >6 NO per cluster.[19]

Multiple RBS-like species were also detected, with the general formula $[Fe_4(S)_3(NO)_x]$, where x is 3-6, along with adducts, including sodium and oxygen (Fig. 4C). The origin of oxygen adducts is not clear, although, we note that under certain conditions aqueous samples may generate oxygen in the ESI source.[25] While an RBS-like $[Fe_4(S)_3(NO)_7]$ species was not observed, an O/Na adduct of $[Fe_4(S)_2(NO)_7]$ was (Table 1). $^{57}Fe/^{34}S$ isotope substitution analysis showed that all of the $[Fe_4(NO)_x(S)_3]$ species were shifted by +10 Da, while the $[Fe_4(S)_2(NO)_7]$ species was shifted by +8 Da (Fig. 4F), consistent with the assignments. All of these species exhibit a similar intensity profile, again increasing above a level of ~6 NO per cluster. The observation of multiple species suggests that some could be due to breakdown of the higher mass species. It is also possible that they might be co-formed, but such species would not be expected to have the same intensity profile. The increasing intensity due to apo-NsrR (mainly as persulfide adducts, Fig. 4A) suggests the instability of the nitrosylation products formed at higher ratios of NO:cluster.

For WhiD, apart from the $[4Fe\text{-}4S](NO)_x$ (x = 1-4) intermediates described above, relatively few iron-nitrosyls were detected, Fig. 5A. Very low amounts of DNIC species (in comparison to NsrR) and no clear RRE-like species were detected, although low amounts of $[Fe_2(NO)_2]S$ and $[Fe_2(NO)_3]S$ were observed (Fig. S6), which may be RRE and/or RBS breakdown products. In the RBS region, small amounts of an RBS-like $[Fe_4(S)_3(NO)_7]$ species were detected, but with essentially none of the $[Fe_4(S)_3(NO)_x]$ species observed for NsrR

apparent. Together with the increasing intensity of the apo-WhiD and persulfide adduct peaks, we conclude that the WhiD iron-nitrosyl species formed beyond the [4Fe-4S](NO)$_4$ species are not stable under the conditions of the non-denaturing ESI-MS experiment.

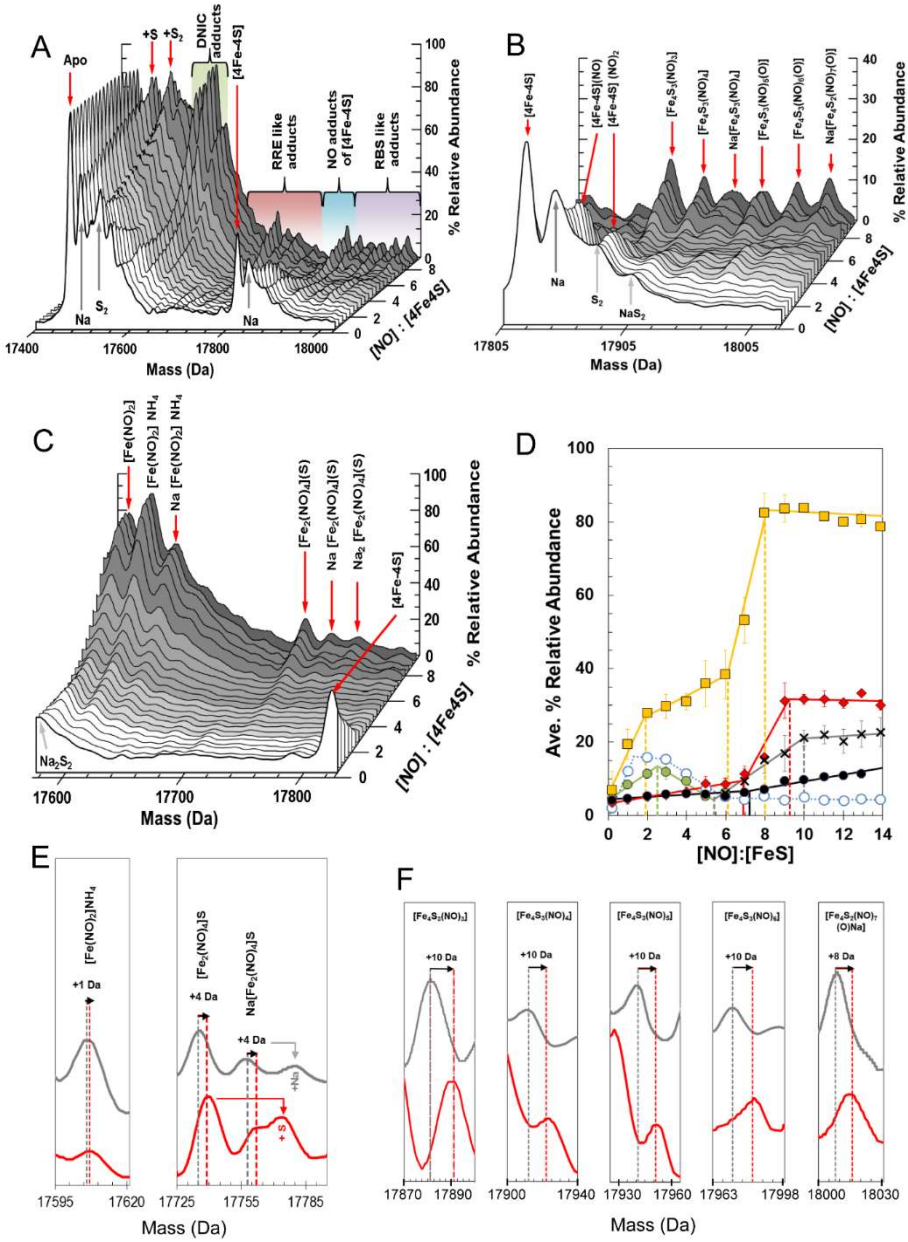

Figure 4. Nitrosylation of [4Fe-4S] NsrR. An aliquot of DTPA NONOate (0.83 mM final concentration) was added to 16 μM [4Fe-4S] NsrR and incubated at 30 °C, releasing 0.39 [NO]:[4Fe-4S] per 5 min. (A) Survey plot showing the formation of new species following exposure to NO, which can be separated into four distinct regions: NO adducts of the [4Fe-4S] cluster, DNIC, Roussin's red (RRE)-like, and Roussin's black (RBS)-like adducts, as indicated. (B) The NO cluster adducts and RBS-like species region is shown in more detail. NO adducts of the [4Fe-4S] cluster were formed at ≤ 3 [NO]:[4Fe-4S], with multiple RBS-like species observed ≥ 6 [NO]:[4Fe-4S]. (C) The DNIC and RRE-like species region is shown in more detail. DNICs formed at low levels of NO and increased simultaneously with RRE-like adducts at [NO]:[4Fe-4S] ≥ 6. (D) Average (n=5) percentage relative abundance of [4Fe-4S](NO) (blue open circles), [4Fe-4S](NO)$_2$ (green circles), DNIC (yellow squares), RRE-like [Fe$_2$(NO)$_4$](S) (red diamonds), [Fe$_4$S$_3$(NO)$_3$] (black crosses), and [Fe$_4$S$_2$(NO)$_7$(O)Na] (black circles) as a function of the [NO]:[4Fe-4S] ratio. Error bars represent standard deviation. (E) Comparisons of nitrosyl species formed in the DNIC and RRE regions during nitrosylation of the natural abundance and ^{57}Fe/^{34}S

substituted forms of [4Fe-4S] NsrR. Left panel shows $[Fe(NO)_2](NH_4)$, which shifts by +1 Da upon isotopic substitution. This ammonium adduct is shown here instead of the $[Fe(NO)_2]$ adduct because of overlap between the $[Fe(NO)_2]$ and Na/S adducts of the apo-protein. Right panel shows $[Fe_2(NO)_4(S)]$ and Na adduct, which both shift by +4 Da. A double persulfide form ($[Fe_2(NO)_4(S)_2]$ is observed clearly in the $^{57}Fe/^{34}S$ NsrR spectrum. (F) As in (E) but for RBS-like species. Panels left to right show: $[Fe_4S_3(NO)_3]$, $[Fe_4S_3(NO)_4]$, $[Fe_4S_3(NO)_5]$, and $[Fe_4S_3(NO)_6]$, which all shift by +10 Da, and $[Fe_4S_2(NO)_7(O)Na]$, which shifts by +8 Da.

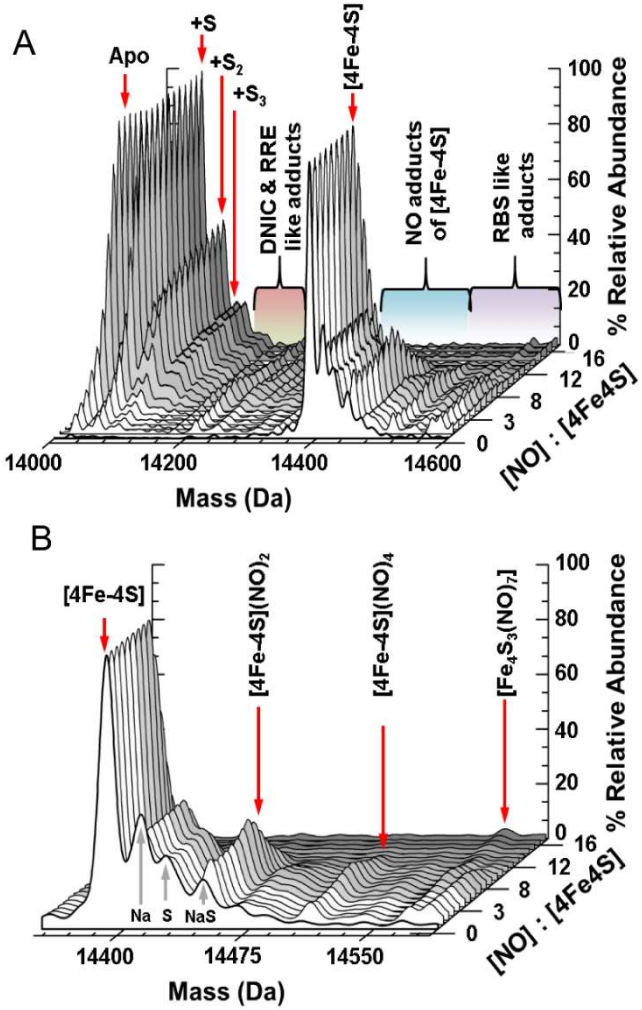

Figure 5. Nitrosylation of [4Fe-4S] WhiD. An aliquot of DTPA NONOate (1.05 mM final concentration) was added to 9.25 μM $^{57}Fe/^{34}S$ substituted [4Fe-4S] WhiD and incubated at 30 °C, releasing 1.4 [NO]:[4Fe-4S] per 2 min. (A) Survey plot showing the formation of new species following exposure to NO. (B) [4Fe-4S] cluster NO adducts and RBS-like species regions in more detail.

Discussion

The reaction of NO with Fe-S clusters is a route of NO toxicity, but also a means by which cells sense environmental changes through reaction with sensor regulators that employ an Fe-S cluster as the sensory module.[2b, 3b, 7, 26] The complexity of reactions of Fe-S clusters with NO have been revealed previously through kinetic and spectroscopic studies[17d, 17e, 20, 27] but the identification of intermediates and products of the reaction have proved extremely difficult due their transient nature and the similar spectroscopic properties of iron-nitrosyl species. An exception to this was the recent detection of NO binding to the human

mitochondrial protein Miner2,[24] but in this case the NO complex was stable and no further reaction was observed. Progress in identifying the products of nitrosylation was made recently through the application of NRVS, which revealed both RRE and RBS-like species for both NsrR and WhiD, with significant amounts of DNIC species also present in NsrR.[18] Furthermore, LC-MS studies of NsrR recently demonstrated the precise nature of the RRE-species formed.[19] However, the identification of intermediate species has remained elusive. Here we have used ESI-MS under non-denaturing conditions, along with Fe/S isotopic substitutions, to probe the reaction of the NO sensing regulators NsrR and WhiD with NO.

The ESI-MS data provides the first unambiguous identification of intermediates in the nitrosylation reactions of regulatory Fe-S cluster proteins. Data for NsrR clearly demonstrate the formation of a single NO complex (+30 Da) of the FeS cluster, [4Fe-4S](NO). For WhiD, a peak at +30 Da was also observed but was less clearly resolved than for NsrR. For NsrR, the mono-nitrosyl was observed to decay away, indicating that a second NO binds relatively easily to the mono-nitrosyl complex, to form a di-nitrosyl, $[4Fe\text{-}4S](NO)_2$, the second intermediate of cluster nitrosylation at +60 Da. This was also clearly detected for WhiD.

Above this ratio of NO:[4Fe-4S], the NsrR and WhiD reaction pathways diverged. For WhiD, a tetra-nitrosyl complex of the FeS cluster, $[4Fe\text{-}4S](NO)_4$, was detected. Studies of the nitrosylation of a site differentiated [4Fe-4S] model complex revealed a tetra-nitrosylated cluster intermediate along the path to RBS formation.[28] In that case, the cluster was extruded from its coordinating tri-thiolate ligand, likely resulting in one NO bound to each iron, as in the $[4Fe\text{-}4S](NO)_4$ complex reported by Gall *et al.*[29] In the case of WhiD, the cluster remained coordinated to the protein, and we propose that this is facilitated by the formation of one or more Cys persulfides that bridge irons in the cluster (Fig. 6).

In general, $[4Fe\text{-}4S](NO)_x$ nitrosylation intermediates of WhiD were observed over a broad range of NO additions, up to 10 NO per cluster, consistent with a more concerted nitrosylation reaction for this protein, in which intermediate species are present at all sub-saturating concentrations of NO but do not sequentially accumulate. Beyond the tetra-nitrosyl intermediate, WhiD iron-nitrosyl products were not stable under the conditions of these experiments, with only low amounts of DNIC and RBS-like species, and some likely RRE/RBS breakdown species observed by ESI-MS.

For NsrR, no further NO adducts of the [4Fe-4S] cluster were observed beyond the $[4Fe\text{-}4S](NO)_2$ complex. This is consistent with previous data from LC-MS showing that persulfide adducts of NsrR begin to accumulate above a level of 2 NO per cluster, indicating that the [4Fe-4S] core begins to break down above this level of NO, with oxidation of released cluster sulfide to sulfane (S^0), which combines with thiols (Cys residues or GSH in this case) to form persulfides. This oxidation process, which also results in a disulfide bond, most likely between Cys93 and Cys99[19] is presumably driven by the formation of iron-nitrosyls, which requires a source of electrons.[17a, 17d]

A range of iron-nitrosyl species were formed in NsrR at higher ratios of NO. DNICs were formed at greatest intensity at ≥6 NO per cluster. Previous solution studies by EPR showed that low levels of DNICS were formed during NO reaction with [4Fe-4S], but these were relatively minor products even at maximum observed intensity at ≥10 NO per cluster, where they accounted for ~16% of the iron originally present.[20] A persulfide bound RRE species and a range of RBS-like species were also observed, though these did not begin to appear at significant intensity until ≥6 NO per cluster. RRE species associated with NsrR were also observed by LC-MS, again only significantly at NO ratios ≥6.[19] For the RBS-like species, the similarity of their formation patterns indicates that they are not formed along a stepwise pathway as a function of NO. Rather, they are formed at the same time, either directly from

the nitrosylation reaction, or as a result of breakdown of an unstable higher mass species during the MS experiment.

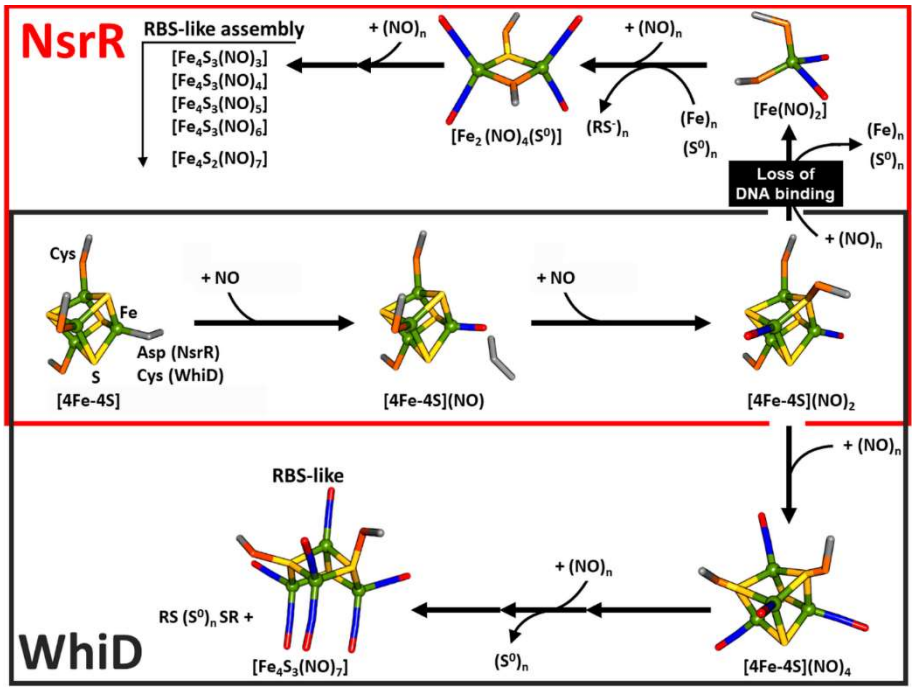

Figure 6. Proposed mechanistic scheme for the nitrosylations of [4Fe-4S] NsrR and WhiD based on ESI-MS data**.** Starting from the [4Fe-4S] cluster form, both regulators follow the same initial path, via mono- and di-nitrosyl complexes (overlapping red and black boxes). The two mechanisms then diverge. For NsrR, the cluster breaks down to form DNIC, RRE and RBS-like species (scheme in red box), with loss of DNA binding above 2 NO per cluster.[20] For WhiD, a $[4Fe\text{-}4S](NO)_4$ species is formed on route to an RBS-like product (scheme in black box). Recent NRVS data showed that RRE-like species are also formed in WhiD,[18] but here ESI-MS showed evidence only for possible RRE breakdown species (and so are not included here). The structures illustrated here for $[4Fe\text{-}4S](NO)_2$, $[4Fe\text{-}4S](NO)_4$, $[Fe_4S_3(NO)_7]$ are speculative, intended to represent chemically reasonable interpretations for the events occurring. Clearly, other possibilities exist. For $[4Fe\text{-}4S](NO)_2$ we propose that NO displaces amino acid side chain ligands for two of the irons, with the free Cys possibly coupling to cluster sulfur to form an iron-bridging persulfide ligand. For $[4Fe\text{-}4S](NO)_4$, we propose the further displacement of Cys by NO and formation of another bridging persulfide ligand, which accounts for how the iron-nitrosyl remains associated with the protein. Cys persulfides are depicted as bridging three irons, but it is more likely that they bridge only two at any one time. Here, for clarity the original Cys sulfur is coloured orange and the sulfide-derived sulfur in yellow but it recognised that these may be scrambled during persulfide formation. For RBS-like $[Fe_4S_3(NO)_7]$, further NO binding to $[4Fe\text{-}4S](NO)_4$ is accommodated at each iron by further loss of sulfur coordination.

Although described as RBS-like species, because of the oxidation of cluster sulfide during Fe-S nitrosylation reactions (three out of four were found to be oxidised during WhiD nitrosylation[17d]), and persulfide adducts were readily detected by LC-MS following [4Fe-4S] NsrR nitrosylation,[19] it is unlikely that these species feature three sulfide bridges. Indeed, the lack of any discernible vibrational shift in the NRVS spectrum upon $^{32}S/^{34}S$ substitution demonstrated that the RBS-like products of NsrR and WhiD nitrosylation do not contain significant amounts of sulfide.[18] It is more likely that these are Cys- or Cys persulfide-bridged forms of an RBS-like species. The ESI-MS data are consistent with this. As indicated in Table 1, the predicted masses of protein-bound forms of RBS-like species cannot be precisely

defined because they depend on the overall charge of the Fe/S/NO adducts, which are unknown. All of the observed masses are within the predicted range, but appear to move towards the lower end of the range as the number of bound NO molecules increases. This is consistent with oxidation of sulfide to S^0, where two negative charges are lost for each sulfide oxidized. We also note that the observed $Fe_4S_2(NO)_7$ species could be related to the novel iron-nitrosyl complex $[Fe_4(\mu_3\text{-}S)_2\text{-}(\mu_2\text{-}NO)_2(NO)_6]^{2-}$, in which two of the NO ligands bridge two irons.[30]

The data presented here show that [4Fe-4S] NsrR and WhiD behave very differently during reaction with NO. The [4Fe-4S] NsrR peak decayed immediately upon reaction with NO and was entirely lost at ~4 NO. In contrast, the WhiD [4Fe-4S] peak remained throughout and was not lost until ≥10 NO per cluster. NsrR intermediate species were observed to form and decay over relatively narrow ratios of NO:[4Fe-4S], whereas WhiD intermediate species formed and persisted over a much wider range of NO concentrations. Thus, for NsrR, NO preferentially reacts with unreacted [4Fe-4S] clusters, leading to detection (but not identification) of intermediates by visible and CD spectroscopies at 2 NO per cluster, with further intermediates at ~4 and ~6 NO per cluster.[20] For WhiD, the reaction is more concerted where clusters that have already undergone reaction with NO preferentially react with further NO towards final product formation.[17d]

The detection of intermediates of Fe-S cluster nitrosylation reactions enables mechanistic proposals for both NsrR and WhiD, see Fig. 6. For both regulators, a mono-nitrosyl complex of the [4Fe-4S] cluster is the first intermediate. For NsrR, the NO is most likely bound at the site-differentiated iron coordinated by Asp8.[4a, 6] For the all-Cys coordinated [4Fe-4S] cluster of WhiD, which iron binds the first NO is not clear. A second NO then binds (at the same or a different iron) to form a di-nitrosyl complex of the [4Fe-4S] cluster. From here, the mechanisms appear to diverge significantly, with the NsrR cluster apparently undergoing disassembly coupled with sulfide oxidation and iron/NO reduction. At least some of the resulting sulfane combines with protein Cys thiols to form persulfides. Cluster disassembly leads to DNIC species and, at higher NO ratios, RRE and RBS-like species begin to accumulate, see Fig. 6. In WhiD, further NO molecules can bind to the cluster di-nitrosyl complex, forming the (likely) tri- and tetra-nitrosyl complexes. Small molecule versions of the tetra-nitrosyl [4Fe-4S] cluster have been reported, including as an intermediate of Fe-S cluster nitrosylation.[28-29, 31] What occurs beyond this step is not so clear, at least from the ESI-MS data. Only small amounts of DNIC were observed, consistent with previous EPR studies that showed much less DNIC species formed in WhiD compared to NsrR,[17d, 20] and only minor amounts of likely RRE breakdown products and some RBS-like species were observed. RRE- and RBS-type species were detected previously by NRVS,[18] consistent with small molecule studies showing that $[4Fe\text{-}4S](NO)_4$ can be converted to RBS under both oxidising and reducing conditions.[28, 31-32] Furthermore, the conversion of both RBS and $[4Fe\text{-}4S](NO)_4$ to DNIC and RRE species has also been reported upon reaction with MeS^-,[31] indicating that interconversion of iron-nitrosyl species can occur readily depending on the redox environment and availability of thiol ligands.

These differences between the nitrosylation mechanisms of NsrR and WhiD are very likely to be physiologically important. Previous kinetic data showed that NsrR reacts more rapidly than WhiD with NO, consistent with its role as a front-line sensor of NO.[20] The ESI-MS data shows that all NsrR clusters will be affected at relatively low NO levels, leading to the formation of stable intermediates. This is key because it was recently shown that binding of [4Fe-4S] NsrR to different promoters was abolished at different ratios of NO:[4Fe-4S] clusters.[20] In the case of the *hmpA2* promoter, binding was abolished at a ratio of NO:[4Fe-

4S] of ≥2, demonstrating that binding is disrupted early in the titration and does not require formation of iron-nitrosyl products similar to the well characterised DNICs, RRE- and RBS-like complexes. The NsrR mechanism appears to have facilitated the evolution of a hierarchical response to NO, with NsrR-promoter DNA complexes exhibiting different sensitivities to NO.[20] For WhiD, the population of [4Fe-4S] WhiD is apparently protected by the more concerted reaction mechanism, meaning that some unreacted [4Fe-4S] clusters remain up to the point when all NO binding is saturated, providing a wider response range for the detection of NO by WhiD.

Experimental Section

Protein purification

His tagged proteins (C-terminal NsrR, N-terminal WhiD) were purified under anaerobic conditions as previously described.[4a, 8c] Protein concentrations were determined by the methods of Smith (Pierce)[33] and Bradford (BioRad),[34] for NsrR and WhiD respectively, with bovine serum albumin as the standard. Cluster content was determined using extinction coefficients at $\varepsilon_{406\ nm}$ of 13.30 (±0.19) mM^{-1} cm^{-1} or 16.36 (±0.04) mM^{-1} cm^{-1} for NsrR or WhiD, respectively.[4a, 8c]

Isotopically enriched clusters

The NifS-catalysed reconstitution of his-tagged proteins was unsuccessful, therefore, to prepare [4Fe-4S] clusters enriched with heavy (^{57}Fe and ^{34}S) isotopes, proteins were initially prepared *in vivo* with ^{57}Fe (Goss Scientific, UK) growth media, as previously described.[27] After purification, samples were buffer exchange into 25 mM HEPES, 2.5 mM $CaCl_2$, 100 mM NaCl 100 mM $NaNO_3$, pH 7.5 via a PD10 column (GE Healthcare). Incorporation of ^{34}S (Goss Scientific Ltd) into the cluster was carried out via sulfide exchange as described by Kennedy *et al.*[35] Briefly, holo- proteins (~70 µM [4Fe-4S]) were treated with an aliquot of ^{34}S sulfide (~27 mM final conc.), DTT (~64 mM final conc.), and incubated at ~46 °C for up to 3 hours. The sample was rapidly cooled to 20 °C, centrifuged to at 14,000 x g for 5 min, and buffer exchanged into a high salt buffer (NsrR: 50 mM Tris, 5% (v/v) glycerol 2 M NaCl, pH 8.0; WhiD: 50 mM Tris, 5% (v/v) glycerol 800 mM NaCl, pH 7.3). Where necessary, centrifugal spin concentrators (Amicon Ultra, 10 K MWCO, regenerated cellulose) were used to reduce the sample volume and concentrate the sample. Control experiments with ^{56}Fe and ^{34}S, confirmed specific enrichment of the [4Fe-4S] cluster with the ^{34}S sulfide isotope. The melting point (T_m) for holo-NsrR was determined, as previously described,[8c] as ~53 ºC, which is similar to the T_m of ~56 ºC previously determined for WhiD,[8c] respectively. The CD spectra of heat treated (including isotopically enriched) samples were identical to non-enriched samples and heat treated NsrR remained competent for DNA binding.

ESI-MS under non-denaturing conditions

Samples for ESI-MS analysis were exchanged into 250 mM ammonium acetate pH 8.0 using Zeba desalting columns (Thermo Scientific) and diluted to ~6 µM cluster (~6 pmol/µl), and infused directly (0.3 ml/hr) into the ESI source of a Bruker micrOTOF-QIII mass spectrometer operating in the positive ion mode. The ESI-TOF was calibrated using ESI-L Low Concentration Tuning Mix (Agilent Technologies, San Diego, CA). Full mass spectra (m/z 500 – 3500) were recorded for 5 min with acquisition controlled using Bruker oTOF Control software, with parameters as follows: dry gas flow 4 L/min, nebuliser gas pressure 0.8 Bar,

dry gas 180 °C, capillary voltage 4500 V, offset 500 V, quadrupole ion voltage 5 V, collision RF 200 Vpp, collision cell voltage 10 V. Processing and analysis of MS experimental data were carried out using Compass DataAnalysis version 4.1 (Bruker Daltonik, Bremen, Germany). Neutral mass spectra were generated using the ESI Compass version 1.3 Maximum Entropy deconvolution algorithm. Exact masses are reported from peak centroids representing the isotope average neutral mass. Mass accuracy was ± 1 Da, which equates to 55 – 75 ppm for the proteins studied here. For apo-proteins, exact masses are derived from m/z spectra, for which peaks correspond to $[M + nH]^{n+}/n$. For cluster- and Fe/S/NO-containing proteins, where the metallo-species contributes charge, peaks correspond to $[M + (FeS/NO)^{x+} + (n-x)H]^{n+}/n$, where M is the molecular mass of the protein, Fe-S is the mass of the particular iron-sulfur cluster of x+ charge, H is the mass of the proton and n is the total charge. In the expression, the x+ charge of the iron-sulfur cluster offsets the number of protons required to achieve the observed charge state (n+).[22] Predicted masses are given as the isotope average of the neutral protein or protein complex, in which cluster- or Fe/S/NO-binding is expected to be charge-compensated.[23, 36]

Nitrosylation of samples for native MS

Initial experiments with aqueous solutions of NO oxide gas resulted in the suppression of protein ionization. Therefore, an MS-compatible NONOate was used as the NO donor.[37] We have previously shown that the nitrosylation of [4Fe-4S] NsrR and [4Fe-4S] WhiD is extremely rapid. Therefore, the slow NO releasing reagent Dipropylenetriamine (DPTA) NONOate (Cayman Chemicals, USA), was chosen for native *in situ* nitrosylation ESI mass spectroscopy experiments. Under these conditions, NO availability limits the reaction, enabling an effective thermodynamic titration of samples with NO. Briefly, an aliquot (up to 0.2 ml) of DPTA NONOate (see figure legends for further details) was added to an aliquot (1.8 ml) of [4Fe-4S] NsrR or WhiD in 250 mM ammonium acetate buffer, maintained at a constant temperature, and infused directly (0.3 ml/hr) into the ESI source, operating in the positive ion mode. Spectra were continuously recorded and averaged every 5 min. DPTA NONOate solutions were prepared immediately before use in 250 mM ammonium acetate pH 8 and quantitated by absorbance, ε_{252nm}= 7000 M^{-1} cm^{-1} (Cayman Chemicals, USA). DPTA NONOate spontaneously dissociates into 2 (±0.1) moles of NO per mole of parent compound, in a pH dependent manner, via a first-order process.[38] In 250 mM ammonium acetate, pH 8, DPTA NONOate decayed with a half-life ($t_{½}$) of 41.8 hrs or 11.0 hrs at 20 °C or 30 °C, respectively. At pH 7.1 the $t_{½}$ was 2.1 hrs at 30 °C. Control experiments with ferrous ammonium sulphate and L-cysteine were followed optically and used to calibrate the time dependent release of NO from DPTA NONOate and concomitant formation of cysteine-DNIC.

Acknowledgements

This work was supported by Biotechnology and Biological Sciences Research Council Grants BB/P006140/1 and BB/L007673/1 and by FeSBioNet COST Action CA15133. We thank UEA for funding the purchase of the Q-TOF instrument.

Conflict of interest

The authors declare no conflict of interest.

Key words: iron-sulfur; nitric oxide; gene regulation; mass spectrometry; nitrosylation

References

[1] R. Bruckdorfer, *Mol Aspects Med* **2005**, *26*, 3-31.

[2] a) B. G. Hill, B. P. Dranka, S. M. Bailey, J. R. Lancaster, Jr., V. M. Darley-Usmar, *J Biol Chem* **2010**, *285*, 19699-19704; b) J. C. Crack, J. Green, A. J. Thomson, N. E. Le Brun, *Acc Chem Res* **2014**, *47*, 3196-3205; c) J. C. Crack, N. E. Le Brun, *Antioxid Redox Signal* **2017** DOI: 10.1089/ars.2017.7369.

[3] a) R. K. Poole, *Biochem Soc Trans* **2005**, *33*, 176-180; b) J. C. Crack, J. Green, A. J. Thomson, N. E. Le Brun, *Curr Opin Chem Biol* **2012**, *16*, 35-44.

[4] a) J. C. Crack, J. Munnoch, E. L. Dodd, F. Knowles, M. M. Al Bassam, S. Kamali, A. A. Holland, S. P. Cramer, C. J. Hamilton, M. K. Johnson, A. J. Thomson, M. I. Hutchings, N. E. Le Brun, *J Biol Chem* **2015**, *290*, 12689-12704; b) N. P. Tucker, M. G. Hicks, T. A. Clarke, J. C. Crack, G. Chandra, N. E. Le Brun, R. Dixon, M. I. Hutchings, *Plos One* **2008**, *3*, e3623; c) E. T. Yukl, M. A. Elbaz, M. M. Nakano, P. Moenne-Loccoz, *Biochemistry* **2008**, *47*, 13084-13092.

[5] N. P. Tucker, N. E. Le Brun, R. Dixon, M. I. Hutchings, *Trends Microbiol* **2010**, *18*, 149-156.

[6] A. Volbeda, E. L. Dodd, C. Darnault, J. C. Crack, O. Renoux, M. I. Hutchings, N. E. Le Brun, J. C. Fontecilla-Camps, *Nat Commun* **2017**, *8*, 15052.

[7] B. K. Kudhair, A. M. Hounslow, M. D. Rolfe, J. C. Crack, D. M. Hunt, R. S. Buxton, L. J. Smith, N. E. Le Brun, M. P. Williamson, J. Green, *Nat Commun* **2017**, *8*, 2280.

[8] a) V. Molle, W. J. Palframan, K. C. Findlay, M. J. Buttner, *J Bacteriol* **2000**, *182*, 1286-1295; b) Jakimowicz, M. R. Cheesman, W. R. Bishai, K. F. Chater, A. J. Thomson, M. J. Buttner, *J Biol Chem* **2005**, *280*, 8309-8315; c) J. C. Crack, C. D. den Hengst, P. Jakimowicz, S. Subramanian, M. K. Johnson, M. J. Buttner, A. J. Thomson, N. E. Le Brun, *Biochemistry* **2009**, *48*, 12252-12264; d) M. J. Bush, G. Chandra, M. J. Bibb, K. C. Findlay, M. J. Buttner, *MBio* **2016**, *7*, e00523-00516.

[9] a) S. H. Kang, J. Huang, H. N. Lee, Y. A. Hur, S. N. Cohen, E. S. Kim, *J Bacteriol* **2007**, *189*, 4315-4319; b) K. Fowler-Goldsworthy, B. Gust, S. Mouz, G. Chandra, K. C. Findlay, K. F. Chater, *Microbiology* **2011**, *157*, 1312-1328.

[10] R. P. Morris, L. Nguyen, J. Gatfield, K. Visconti, K. Nguyen, D. Schnappinger, S. Ehrt, Y. Liu, L. Heifets, J. Pieters, G. Schoolnik, C. J. Thompson, *Proc Natl Acad Sci U S A* **2005**, *102*, 12200-12205.

[11] N. Banaiee, W. R. Jacobs, J. D. Ernst, *Infect Immun* **2006**, *74*, 6449-6457.

[12] J. Daniel, C. Deb, V. S. Dubey, T. D. Sirakova, B. Abomoelak, H. R. Morbidoni, P. E. Kolattukudy, *J Bacteriol* **2004**, *186*, 5017-5030.

[13] a) A. Singh, D. K. Crossman, D. Mai, L. Guidry, M. I. Voskuil, M. B. Renfrow, A. J. C. Steyn, *Plos Pathog* **2009**, *5,* e1000545; b) A. Singh, L. Guidry, K. V. Narasimhulu, D. Mai, J. Trombley, K. E. Redding, G. I. Giles, J. R. Lancaster, A. J. C. Steyn, *Proc Natl Acad Sci USA* **2007**, *104*, 11562-11567.

[14] L. J. Smith, M. R. Stapleton, G. J. M. Fullstone, J. C. Crack, A. J. Thomson, N. E. Le Brun, D. M. Hunt, E. Harvey, S. Adinolfi, R. S. Buxton, J. Green, *Biochem J* **2010**, *432*, 417-427;

[15] M. J. Bush, *Mol Microbiol* **2018**, doi: 10.1111/mmi.14117.

[16] A. R. Butler, C. Glidewell, M. Li, *Adv Inorg Chem* **1988**, *32*, 335-393.

[17] a) T. C. Harrop, Z. J. Tonzetich, E. Reisner, S. J. Lippard, *J Am Chem Soc* **2008**, *130*, 15602-15610; b) C. E. Tinberg, Z. J. Tonzetich, H. Wang, L. H. Do, Y. Yoda, S. P. Cramer, S. J. Lippard, *J Am Chem Soc* **2010**, *132*, 18168-18176; c) Z. J. Tonzetich, H. Wang, D. Mitra, C. E. Tinberg, L. H. Do, F. E. Jenney, Jr., M. W. Adams, S. P. Cramer, S. J. Lippard, *J Am Chem Soc* **2010**, *132*, 6914-6916; d) J. C. Crack, L. J. Smith, M. R. Stapleton, J. Peck, N. J. Watmough, M. J. Buttner, R. S. Buxton, J. Green, V. S. Oganesyan, A. J. Thomson, N. E. Le Brun, *J Am Chem Soc* **2011**, *133*, 1112-1121; e) J. C. Crack, M. R. Stapleton, J. Green, A. J. Thomson, N. E. Le Brun, *J Biol Chem* **2013**, *288*, 11492-11502.

[18] P. N. Serrano, H. Wang, J. C. Crack, C. Prior, M. I. Hutchings, A. J. Thomson, S. Kamali, Y. Yoda, J. Zhao, M. Y. Hu, E. E. Alp, V. S. Oganesyan, N. E. Le Brun, S. P. Cramer, *Angew Chem Int Ed Engl* **2016**, *55*, 14575-14579.
[19] J. C. Crack, C. J. Hamilton, N. E. Le Brun, *Chem Commun* **2018**, *54*, 5992-5995.
[20] J. C. Crack, D. A. Svistunenko, J. Munnoch, A. J. Thomson, M. I. Hutchings, N. E. Le Brun, *J Biol Chem* **2016**, *291*, 8663-8672.
[21] a) N. Morgner, C. V. Robinson, *Curr Opin Struct Biol* **2012**, *22*, 44-51; b) C. Schmidt, C. V. Robinson, *The FEBS J* **2014**, *281*, 1950-1964.
[22] K. A. Johnson, M. Verhagen, P. S. Brereton, M. W. W. Adams, I. J. Amster, *Anal Chem* **2000**, *72*, 1410-1418.
[23] J. C. Crack, A. J. Thomson, N. E. Le Brun, *Proc Natl Acad Sci USA* **2017**, *114*, E3215-E3223.
[24] Z. Cheng, A. P. Landry, Y. Wang, H. Ding, *J Biol Chem* **2017**, *292*, 3146-3153.
[25] S. Banerjee, S. Mazumdar, *Int J Anal Chem* **2012**, 282574. DOI: 10.1155/2012/282574
[26] H. G. Ding, B. Demple, *Proc Natl Acad Sci U S A* **2000**, *97*, 5146-5150.
[27] J. C. Crack, J. Green, A. J. Thomson, N. E. Le Brun, *Meth Mol Biol* **2014**, *1122*, 33-48.
[28] E. Victor, S. J. Lippard, *Inorg Chem* **2014**, *53*, 5311-5320.
[29] R. S. Gall, C. T. W. Chu, L. F. Dahl, *J Am Chem Soc* **1974**, *96*, 4019-4023.
[30] S. W. Yeh, C. C. Tsou, W. F. Liaw, *Dalton Trans* **2014**, *43*, 9022-9025.
[31] A. R. Butler, C. Glidewell, A. R. Hyde, J. C. Walton, *Polyhedron* **1985**, *4*, 797-809.
[32] C. T. W. Chu, F. Y. K. Lo, L. F. Dahl, *J Am Chem Soc* **1982**, *104*, 3409-3422.
[33] P. K. Smith, R. I. Krohn, G. T. Hermanson, A. K. Mallia, F. H. Gartner, M. D. Provenzano, E. K. Fujimoto, N. M. Goeke, B. J. Olson, D. C. Klenk, *Anal Biochem* **1985**, *150*, 76-85.
[34] M. M. Bradford, *Anal Biochem* **1976**, *72*, 248-254.
[35] M. C. Kennedy, M. H. Emptage, H. Beinert, *J Biol Chem* **1984**, *259*, 3145-3151.
[36] K. L. Kay, C. J. Hamilton, N. E. Le Brun, *Metallomics* **2016**, *8*, 709-719.
[37] E. Rivera-Tirado, M. Lopez-Casillas, C. Wesdemiotis, *Rapid Commun Mass Sp* **2011**, *25*, 3581-3586.
[38] C. M. Maragos, D. Morley, D. A. Wink, T. M. Dunams, J. E. Saavedra, A. Hoffman, A. A. Bove, L. Isaac, J. A. Hrabie, L. K. Keefer, *J Med Chem* **1991**, *34*, 3242-3247.

Table of contents graphic

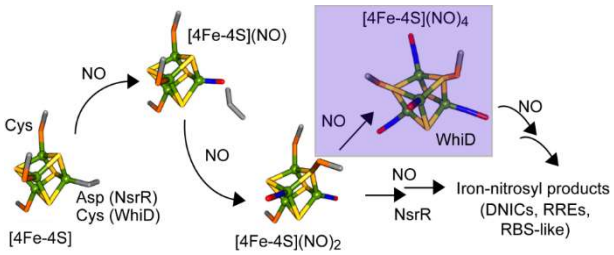

In biology, nitric oxide is both a toxin and a signalling molecule, and reactions with iron-sulfur cluster proteins are relevant to both. Non-denaturing mass spectrometry reveals iron-nitrosyl species of the type [4Fe-4S](NO)$_x$ as intermediates of the nitric oxide-sensing reactions of the [4Fe-4S] cluster-containing transcriptional regulators NsrR and WhiD. The data also reveal a clear mechanistic distinction between these two regulators.